

## **EXPERIMENT vs. THEORY IN SOLID-STATE REACTION KINETICS: A discrete model for $\text{NH}_4\text{HCO}_3$ thermal decomposition**

*A. Korobov*\*

V. N. Karazin Kharkov National University, P.O. Box 10313, 61023 Kharkov, Ukraine

(Received September 22, 2002; in revised form May 14, 2003)

### **Abstract**

A discrete model has been constructed for the thermal decomposition of  $\text{NH}_4\text{HCO}_3$  single crystals according to the mechanism of nucleation and growth to impingement. The rate-time curve has been computed in terms of the crystal structure of ammonium hydrocarbonate proceeding from microscopic assumptions. This illustrates previously suggested discrete approach to solid-state reaction kinetics in terms of Dirichlet tessellations.

**Keywords:** crystal structure, crystolysis reactions, kinetic models, negative crystals, planigons, random tessellations, topochemical reactions

### **Introduction**

Reactions that proceed within a crystalline matrix in such a way that this matrix is disintegrated are dealt with in this paper. The word combination ‘solid-state reactions’ is used for them in accordance with practice, but it should be recognized that this term is too broad. It is also used, for instance, for reactions between very active species isolated in an inert (e.g. argon) matrix. The need is felt to make words more precise. An original crystal plays simultaneously two roles, the role of the reactant and the role of the medium in which the considered reaction proceeds. This medium is disintegrated in the course of a reaction. Obviously, there are no analogs in other fields of chemical kinetics. This feature is neatly emphasized by the term ‘crystolysis’ [1]. Another specific term used for this class of reactions is ‘topochemical reactions’ [2]. It emphasizes the fact, also very important, that reactions under discussion proceed at the interface. It seems reasonable to mention both terms as key words to facilitate the electronic search.

Kinetics of crystolysis reactions seems to be the field of physical chemistry in which the gap between theory and experiment is the biggest, theory lagging behind experiment. To reduce this gap, a discrete approach to crystolysis reaction kinetics has been suggested. Its main points have been discussed in detail [3–7], but these pa-

---

\* Author for correspondence: E-mail: Alexander.I.Korobov@univer.kharkov.ua

pers lack particular examples. The present paper complements them and aims to illustrate the main ideas and mathematical conceptions of the approach suggested in the framework of a particular example.

### **Example: $\text{NH}_4\text{HCO}_3$**

The choice of the example is determined by the following considerations.

One of the main points of the approach suggested is that a solid reagent must be represented in kinetic models in terms of its crystal structure. The first step of any decomposition is the disintegration of this structure with the redistribution of chemical bonds and release of species that form new phase(s) as further steps. In mathematical models currently in use, this step is not reflected properly. If, for example, the rate of thermal decomposition of calcium carbonate is described using the Avrami–Erofeev rate equation, this model implies formation of nuclei of the new phase and their growth to impingement. This means that both the original phase disintegration and the new phase formation are described together, though they may not be coherent (and in the majority of cases are not coherent). To emphasize this lack of coherence, we use as an example a reaction that proceeds according to a mechanism of nucleation and growth to impingement, with the formation of gaseous products only. Such a reaction is the thermal decomposition of  $\text{NH}_4\text{HCO}_3$ .

Once we are interested in details of the disintegration of the crystal structure, we need experimental data for single crystals. One of the main reasons for choosing  $\text{NH}_4\text{HCO}_3$  as an example is the existence of experimental data for single crystals prepared as carefully as for X-ray analysis [8–11]. We will refer to experimental data for  $\text{NH}_4\text{HCO}_3$  single crystals grown during 7 days at 7 to 10°C. In contrast to crystals selected from a commercial batch, or quickly recrystallized, carefully prepared single crystals demonstrate in thermal decomposition the so-called crystallographic correspondence (or crystallographic factor), which means that thermal decomposition figures (rhombus) correspond to the crystal structure of  $\text{NH}_4\text{HCO}_3$ . Decomposition figures of irregular form observed for quickly recrystallized crystals [9] are an example of the lack of crystallographic correspondence.

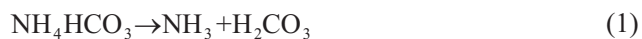
In homogeneous kinetics the routine is to carry out a reaction in the kinetic regime if the mechanism is under study; in the diffusion or mixed regime the mechanism cannot be revealed. The same is the case for crystallysis reactions. But these reactions are more involved, and in addition to the kinetic regime the crystallographic correspondence needs to be provided for subtler insight into the mechanism. According to [12], the crystallographic correspondence may be achieved in many cases if crystals are prepared carefully and reaction conditions are mild enough. For  $\text{NH}_4\text{HCO}_3$  single crystals this is convincingly demonstrated [8–11]. Unfortunately, such a careful preparation of crystals currently is far from being the common practice in solid-state reaction kinetics.

In addition to crystallographic correspondence, one more advantageous peculiarity of the chosen example is that only one crystal face, (001), enters the reaction because  $\text{NH}_4\text{HCO}_3$  single crystals are plate-like. Approximate dimensions of (001) face of crystals used are 20×5 mm [8]. When the thermal decomposition proceeds in the kinetic re-

gime, rhombic figures oriented in one and the same manner are observed: the longer diagonal of each rhomb is oriented in [010] direction [11]. The kinetic region is above 60°C [8, 11]; at lower temperatures the reaction proceeds in the diffusive region and the mechanism is different. If a relatively small number of nuclei is formed at the (001) crystal face and the reaction has time to proceed considerably into the bulk, rhombic holes are observed [9, 12]. This is the clearest example of negative crystals that appear and evolve according to the model of nucleation and growth to impingement.

It is also important that kinetic data obtained microscopically and gravimetrically agree; the conclusion is that the visually observed front coincides with the reaction interface [10]. Generally, this may not be the case [12]. One more detail advantageous in the present context is that according to X-ray and IR data no intermediate phases are formed in the course of the reaction.

All three reaction products retard the reaction, but the influence of NH<sub>3</sub> is greatest [9]. On this basis it was suggested that NH<sub>4</sub>HCO<sub>3</sub> decomposes into NH<sub>3</sub> and H<sub>2</sub>CO<sub>3</sub>. But this idea received at that time no theoretical support. Now, when the kinetic stability of H<sub>2</sub>CO<sub>3</sub> has been shown both experimentally and theoretically [13], the validity of that suggestion causes practically no doubt. This is one of the main reasons for selecting this reaction as the example: chemical elementary event to be described by kinetic models is the proton transfer



The most representative features of the chosen example are as follows:

- The reactant is a carefully prepared single crystal with only one face entering the thermal decomposition reaction.
- The chemistry of the thermal decomposition is simply proton transfer, and only gaseous products are formed. The reaction is not complicated by intermediate phases or numerous phase transitions.
- The reaction proceeds according to a mechanism of nucleation followed by growth to impingement with the formation of rhombic negative crystals the form of which corresponds to the crystal structure of NH<sub>4</sub>HCO<sub>3</sub>

Perhaps, this is one of the simplest examples that a theorist may find within the discussed class of reactions as a model one. The aim of this paper is to follow, step-by-step, the pass from the crystal structure of ammonium hydrocarbonate to a discrete kinetic model of its thermal decomposition.

## Discrete model

A discrete model for NH<sub>4</sub>HCO<sub>3</sub> thermal decomposition will be constructed in terms of Dirichlet tessellations, planigons and random tessellations. Planigon theory [14, 15] is new for chemical kinetics but is used in crystallography [16]. Random tessellations [17] are new for chemistry (though successfully used in biology, astronomy, geography, etc). All related mathematical conceptions have been explained in [3–7] and their advantages in the context of solid-state reaction kinetics have been discussed. The aim of this section

is to illustrate the approach suggested on a particular example. Accordingly, only very brief explanations of mathematical tools are given.

#### *NH<sub>4</sub>HCO<sub>3</sub> crystal structure*

The crystal structure of NH<sub>4</sub>HCO<sub>3</sub> was reported in [18]. Crystals of NH<sub>4</sub>HCO<sub>3</sub> belong to the rhombic system; the space group is Pccn; parameters of the unit cell are:  $a=7.255$  Å,  $b=10.709$  Å,  $c=8.746$  Å. For purposes of this paper the crystal structure may be represented as being composed of separate NH<sub>4</sub> tetrahedra and (HCO<sub>3</sub>)<sub>n</sub> chains shown in Fig. 1a. This figure is a schematic representation of the crystal structure, not the molecular structure. With this in mind, lines between atoms should be understood as direct contacts between atoms rather than covalent or hydrogen bonds. Chains are situated along the  $c$ -axis. Each CO<sub>3</sub> fragment is a plate and its declination from the  $bc$ -plane is  $\pm 20^\circ$ ; positive and negative declinations alternate along the chain. There are three types of oxygen atoms in the structure. Each oxygen atom of type 1 (Fig. 1a) has one short contact (0.913 Å) with a hydrogen atom of the chain (solid line in the figure); each oxygen atom of type 2 has one long contact (1.693 Å) with a hydrogen atom of the chain (dotted line); each oxygen atom of type 3 has no contacts with hydrogen atoms of the chain. Two adjacent chains differ in orientation, and also carbon atoms are shifted along  $c$ -axis. The third chain of the structure completely repeats the first one.

(HCO<sub>3</sub>)<sub>n</sub> chains are linked by NH<sub>4</sub> tetrahedra, which have no direct contacts between themselves (Fig. 1b). Each NH<sub>4</sub> tetrahedron is linked with four different (HCO<sub>3</sub>)<sub>n</sub> chains: one contact with one chain. In Fig. 1b nitrogen atoms are situated above carbon atoms, and two hydrogen atoms of each tetrahedron are free for contacts with two more chains. Note that oxygen atoms of type 1 have no contacts with NH<sub>4</sub> tetrahedra. Each oxygen atom of type 2 has one contact with NH<sub>4</sub> tetrahedra. Each oxygen atom of type 3 has three contacts with different NH<sub>4</sub> tetrahedra; only two of them are shown in Fig. 1b, the third one being with a NH<sub>4</sub> tetrahedron situated below the C-C plane.

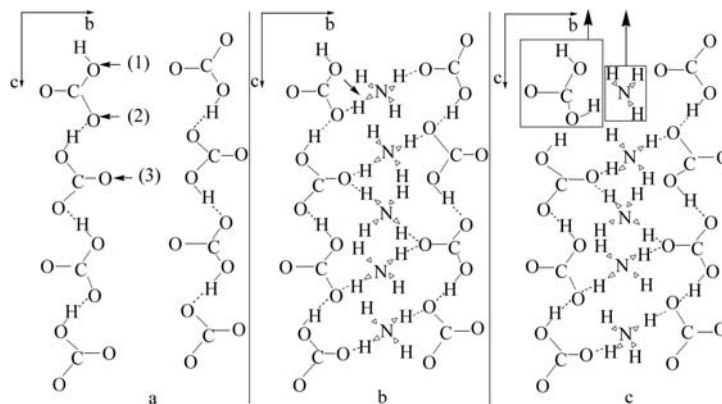


**Fig. 1** Crystal structure of NH<sub>4</sub>HCO<sub>3</sub> as viewed along  $a$ -axis: a – two (HCO<sub>3</sub>)<sub>n</sub> chains; b – NH<sub>4</sub> tetrahedrons are added; c – proton transfer with the escape of two molecules into gaseous phase

It follows that each  $\text{NH}_4$  tetrahedron has three contacts with oxygen atoms of type 3 and one contact with oxygen atom of type 2. Accordingly, it is reasonable to assume for symmetry considerations, that the latter atom is transferred in the thermal decomposition reaction. This is illustrated in the upper part of Fig. 1c. As will be shown below, this assumption agrees with the localized character of the decomposition and the form of decomposition figures. More arguments in its favour are given in [19] where the use is made of the benefit of numerous color illustrations.

The most developed crystal face of  $\text{NH}_4\text{HCO}_3$  single crystals, which enters the reaction, is perpendicular to the  $(\text{HCO}_3)_n$  chains. It cannot be represented in a way similar to Fig. 1. Figure 2a schematically shows the projection of the crystal structure onto the (001) face, constructed using atomic coordinates for  $\text{NH}_4\text{HCO}_3$  [18] and coordinates of equivalent positions for the Pccn group [20]. The symmetry group of this projection is c2mm; cell parameters  $a'=a$  and  $b'=b$ ; the coordinate origin is at  $1/4, 1/4, z$  [20]. In Fig. 2 hydrogen atoms of  $(\text{HCO}_3)_n$  chains are not shown for simplicity.

Within the approach suggested a single crystal is described as the set of crystallographic planes parallel to the chosen crystal face [3, 21]. The exposition of this approach convenient in the present context may be found, for example, in [22]. In these terms, Fig. 2a represents the irreducible crystal plate, which is the set of four crystallographic planes parallel to (001) face that exhaust all possible projections onto this face. Note the following details of this figure. There are two types of nitrogen atoms: those shown in white are situated higher and those shown in gray are situated lower. The same is the case for carbon atoms: white atoms are situated higher than black ones. Light gray oxygens are oxygens of type 2; dark gray oxygens are oxygens of type 3. Oxygens of type 1 are projected practically at the same points as oxygens of

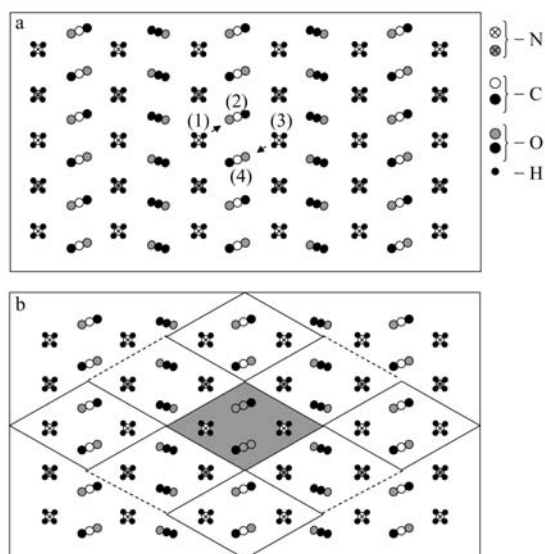


**Fig. 2** Projection of the  $\text{NH}_4\text{HCO}_3$  crystal structure onto (001) face: a – two conjugated  $\text{NH}_4$ - $\text{HCO}_3$  pairs are shown; b – planignon tessellation

type 2. The situation of light and dark gray oxygens alternates along the row. More details of the surface structure are shown in color figures of [19].

#### *From the crystal structure to kinetic models*

Note that the effect of the reactant crystallography on the surface nucleation and the advancement of reaction interface has been examined for a number of decomposition reactions ([23] for review). But this information is not incorporated into kinetic model functions in terms of the crystal structure of a solid reactant. As a result, it is poorly used in quantitative kinetic data analysis. To overcome this gap is one of the main aims of the approach suggested [3–5]. In this section, the conversion-time curve for the  $\text{NH}_4\text{HCO}_3$  thermal decomposition will be computed in terms of the described crystal structure proceeding from the above proton transfer assumption.

#### *Nucleation (1)*

It is commonly agreed that this stage is the most controversial one. It is difficult to investigate both experimentally and theoretically. The cited publications on  $\text{NH}_4\text{HCO}_3$  thermal decomposition are not an exception in this respect: very little attention is paid to nucleation. Generally nuclei are formed at defects of the crystal structure; defects are random and disparate. Within approach suggested, relevant issues convenient to discuss after the unrestricted growth in terms of planigons will be introduced. To postpone this discussion, we will adopt as the zero approximation the most simple model situation: there are no surface imperfections and the reaction starts due to proton transfer as the result of its fluctuation. Later we will return to more realistic situations.

Suppose that a proton has passed from the  $\text{NH}_4$  tetrahedron (1) in Fig. 2a to the oxygen atom of type 2 of  $\text{HCO}_3$  group (2) as a result of a fluctuation. Note that this is the only proton of this  $\text{NH}_4$  tetrahedron that may transfer according to the above assumption. This transfer is followed by the escape of corresponding  $\text{NH}_3$  and  $\text{H}_2\text{CO}_3$  molecules into the gaseous phase. As a result, the  $\text{HCO}_3$  group (4) will be disturbed which also has direct contact with the  $\text{NH}_4$  tetrahedron (1), but via the oxygen atom of type 3; two other contacts being with deeper groups. It is reasonable to expect that this group will take the corresponding proton from the  $\text{NH}_4$  tetrahedron (3), which in turn also has direct contact with the  $\text{HCO}_3$  group (2) via the oxygen atom of type 3 and, accordingly, will also be disturbed upon escape of this group. Thus, it is unlikely that groups (1) and (2) will pass to the gaseous phase without groups (3) and (4). We will consider the discussed groups as two conjugated  $\text{NH}_4 - \text{HCO}_3$  pairs that simultaneously pass into the gaseous phase as a result of a fluctuation, thus giving birth to a model nucleus of the negative crystal.

#### *Planigon tessellations*

Planigons are fundamental regions of two-dimensional Fedorov groups [16]. The theory of planigons has been developed by Delone *et al.* [14] and by Grunbaum and Shephard [15]. Various aspects of their use in describing the crystallysis reaction ki-

netics and relevant mathematical conceptions have been discussed in [3, 24]. In brief, main advantages of planigons in comparison with the more familiar language of crystal lattices are as follows. An extensional measure may be put into correspondence to an atom or group of atoms. The description of the crystal structure in terms of planigons is more detailed because the combinatorial-topological net is taken into account along with the symmetry [14]. This means that several types of planigons correspond to the same two-dimensional symmetry group. This more detailed description is adequate to the wide variety of the observed localization figures. For each planigon, adjacent planigons may be pointed out. Below this is used in moving from the geometry of the crystal structure to the decomposition kinetics.

The transition from the  $\text{NH}_4\text{HCO}_3$  crystal structure to planigon tessellations is as follows. The space group of  $\text{NH}_4\text{HCO}_3$  is Pccn [18]. The two-dimensional group of the projection of the crystal structure onto the (001) face (shown in Fig. 2) is c2mm [20]. As many as eight types of planigons correspond to this group: two general types and six special types [14]. In addition to the symmetry group, the choice of the planigon type depends on the cell parameters and on the system of points for which the planigon tessellation is constructed. This may be a set of particular symmetrically equivalent atoms or groups of atoms, but may be a set of any other uniquely defined symmetrically equivalent points. According to the above nucleation assumption, it is reasonable to construct the planigon tessellation for centers of conjugated  $\text{NH}_4\text{-HCO}_3$  pairs. In this case planigon type  $P_{4A,23}$  (from tables in [14]) is relevant. A piece of corresponding planigon tessellation is shown in Fig. 2b.

#### *Reaction interface*

Reactions of the type discussed occur at the reaction interface. Langmuir substantiated this statement using the rule of contraries: otherwise solid solutions would be formed instead of separate phases [25]. This is a purely macroscopic explanation of the localization phenomena. In conventional kinetic models the reaction interface is represented as a surface without thickness which separates two phases, and particular atoms or groups of atoms are not represented. To make a model chemically meaningful means to explain the localization phenomena in terms of elementary events. For this, a more detailed representation of the reaction interface is required.

A reaction is localized at the interface due to enhanced reactivity of interface atoms or groups of atoms. These atoms are said to be in the reaction situation. Also, we will say, for simplicity, that a planigon has entered the reaction if atoms contained in that planigon have entered the reaction. To a considerable extent, the local increase of reactivity is the result of the disruption of the crystal lattice. Suppose that the gray planigon in Fig. 2b has entered the reaction, i.e. atoms represented by this planigon have passed to the gaseous phase as described above. As a consequence, eight neighboring planigons appear to be in the reaction situation.  $\text{NH}_4\text{-HCO}_3$  pairs contained in these planigons have a higher probability of entering the reaction as a result of being disturbed by the disruption of the crystal lattice. These eight planigons form the reaction zone. In these terms the localized advance of the reaction interface may be described.

### Unrestricted advance of the reaction interface

The unrestricted advance of the reaction interface occurs until the first impingement with a neighboring growing negative crystal. The advance along the surface is described in terms of planigons; the advance into the bulk is described layer-by-layer [3, 21]. This means that the description is 2-dimensional+1-dimensional.

For the particular example discussed, the description is as follows. In the direction perpendicular to the (001) face, the crystal is subdivided into irreducible crystal plates, each being represented by the planigon tessellation. Two of them are shown in Fig. 3. The first step for plate 1 is a planigon in the reaction situation (Fig. 3a). At the next step this planigon enters the reaction, and eight more planigons appear to be in the reaction situation, i.e. form the reaction interface (Fig. 3b). At this step the reaction interface is propagated (or transmitted) to these eight planigons. An equal probability is assumed for them to enter the reaction at the next step. Strictly speaking, these planigons are not completely equivalent: four of them represent the same crystal layer as the starting planigon, whereas four others (which have one dotted edge in Fig. 2b) represent the lower crystal layer. But still all of them represent the same irreducible plate, and here we will not distinguish them. This is a possibility for further detailing the model in the future. At step 3, eight planigons enter the reaction and the reaction interface propagates towards sixteen more planigons. Also, at this step, the central planigon of the second irreducible plate comes to light and appear to be in the reaction situation. This means that the reaction interface is propagated towards the second plate, and further events within the second plate will repeat the events described within the first plate. Thus described decomposition is localized within the reaction interface. The decomposition figure is a rhomb with the ratio of diagonals 1.467. Before nuclei impinge (or intersect), their boundaries move with practically constant rate [10, 11]. At the temperature 80°C and pressure  $10^{-2}$  Pa the microscopically registered rate along the bigger diagonal is  $v_1=120\pm 20\cdot 10^{-5}$  mm min<sup>-1</sup>; the rate along the smaller diagonal is  $v_2=81\pm 10\cdot 10^{-5}$  mm min<sup>-1</sup> [10]. The ratio of rhomb diagonals agrees well with the ratio  $v_1/v_2=1.482$ .

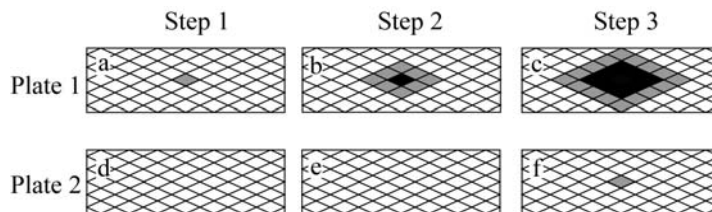


Fig. 3 First steps of the reaction interface advance in terms of planigons

Step  $s$  in this description is a discrete variable that stands for time. Planigons representing each step at the reaction interface form a concentric belt around planigons that have entered the reaction. It was shown in [21] that generally the unrestricted growth in terms of planigons is describable by second-order difference equations. In this particular case the equation of the unrestricted growth is very simple:

$$n(s)=8s+1 \quad (2)$$



where  $n(s)$  is the number of planigons in the concentric belt at step  $s$ ;  $s$  is counted off zero;  $s=0$  corresponds to the formation of nucleus. Remind that each planigon contains two conjugated  $\text{NH}_4 - \text{HCO}_3$  pairs. The relationship of  $n(s)$  to the degree of conversion will be discussed below. The relationship of  $s$  to actual time is as follows. At each step the advance of the reaction front is  $10.7 \cdot 10^{-8}$  cm along the bigger diagonal and  $7.3 \cdot 10^{-8}$  cm along the smaller diagonal, which follows from the above cell parameters. Comparison of these figures with  $v_1$  and  $v_2$  show that one step takes  $\sim 10^{-2}$  s.

### Nucleation (2)

To simplify the picture, we started with an unrealistic assumption about the nucleation. Nuclei are formed at defects of the crystal structure that are random in their situation, orientation and the number of atoms (planigons) involved. The central issue here is whether these random nuclei may evolve with time into regular negative crystals oriented in one and the same manner. To approach this issue cellular automata on planigon tessellations have been introduced [3, 21, 26]. They provide the possibility to describe the transformation of random irregular nuclei into regular symmetric figures with subsequent stable growth. Rules may be formulated according to which nuclei different in the number of planigons, form and orientation, evolve into the same regular figure.

In Fig. 4 all possible 2-nuclei (i.e. nuclei consisted of two planigons) are shown for the example discussed. There are three possible nuclei. Consider the planigon tessellation as a cellular automation and introduce the following simple rule.

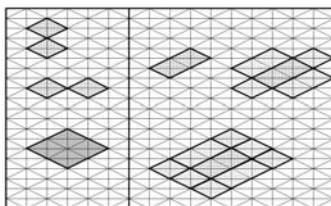


**Fig. 4** All possible 2-nuclei and first steps of their evolution in terms of planigons

Two values,  $c=0$  and  $c=1$ , are possible for each planigon;  $c=0$  means that planigon has not yet entered the reaction,  $c=1$  means that planigon has entered the reaction.

If a planigon with the value  $c=0$  has at its boundary two planigons with the value  $c=1$ , the reaction is propagated towards it first of all.

If each of boundary planigons with  $c=0$  have one common edge with the growing negative crystal, the interaction is propagated simultaneously towards all these planigons.

For 1-nucleus this rule provides the unrestricted growth shown in Fig. 3. The same is the case for two of three 2-nuclei shown in the left part of Fig. 4. The third 2-nuclei, shown in the right part of Fig. 4, evolves into a parallelogram (first two steps are shown). But note that this parallelogram only slightly differs from the rhombus, and in microscopic observations these two figures are difficult to distinguish. It may be shown in the same manner that there are eight 3-nuclei: four evolve into

rhombus and four others evolve into parallelograms. Therefore, starting from different nuclei, we ultimately arrive at the stable growth of regular negative crystals as described in the previous section. An advantage of this approach is that the evolution of a random nucleolus into a regular negative crystal and further evolution of this regular negative crystal until the impingement with a neighbour are described in one and the same terms. Within conventional geometric-probabilistic approach this is not the case. Widely used nucleation laws (instantaneous nucleation, constant intensity of nucleation, etc.) concern critical nuclei that must be of the same form and orientation. Otherwise, the applicability conditions will be violated [27]. The way in which sub-critical nuclei evolve into stable ones is not tractable within conventional approach. This point is discussed in detail in [4].

#### *Restricted advance of the reaction interface*

As nuclei grow, they impinge (or intersect). This stops their growth in the direction of the contact, the growth in other directions being unchanged. These impingements of randomly situated nuclei, generally of different age, determine the actual extension of the reaction interface, to which the reaction rate is proportional. The picture obtained after the process has been completed is termed the random tessellation [17]. In some cases the random tessellation may be directly observed. An example is a carefully polished metallographic lapping. But this possibility is an exception rather than the rule. Mathematical aspects of random tessellations are the subject of stochastic geometry [28].

In Fig. 5 a very small piece of a random tessellation is sketched for the (001) face of  $\text{NH}_4\text{HCO}_3$  single crystal. There are 7 nuclei in this figure shown in black. Again, for simplicity each nucleus consists of one planigon. To construct the random tessellation for them means to subdivide the plane into domains in such a way that all planigons of the given domain will be closer to one of the nuclei than to any other. This nucleus is termed the centre of action for this domain. In relating a particular planigon to one or another nucleus, the distance is measured in the number of steps required a growing nucleus to reach this planigon. This means that the metric is determined by the  $\text{NH}_4\text{HCO}_3$  crystal structure and differs from the Euclidian one. Some planigons are equidistant from two nuclei. These are planigons at which impingements of growing nuclei occur, and they form boundaries of domains. In Fig. 5 these planigons are shown in grey. Only one domain of the central nucleus is shown in the figure completely. This domain may be considered as the nucleus that has grown

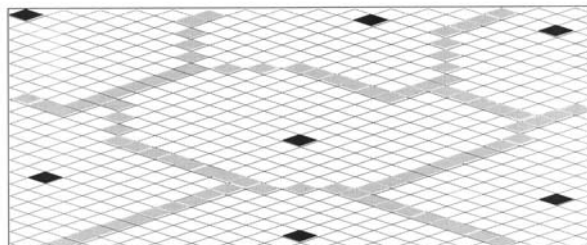


**Fig. 5** A piece of discrete non-Euclidian random tessellation on the (001) crystal face of  $\text{NH}_4\text{HCO}_3$

completely. Alternatively, it may be considered as the domain that will be occupied in the long run by the growing nucleus [6]. In this case function  $N(s)$  may be associated with this domain, where  $N$  is the number of planigons constituting the growing nucleus at step  $s$ . If  $N_0$  is the total number of planigons constituting the domain, then  $a(s)=N(s)/N_0$  is the degree of conversion for this domain.  $N(s)$  and  $a(s)$  functions for the central domain in Fig. 5 are given in Table 1 ( $N_0=139$ ). Of course, Fig. 5 is a schematic representation for which these functions may be easily calculated by hand. Far more steps are required in reality for a nucleus to reach boundaries of the domain. The sum of  $a(s)$  functions for all domains of the random tessellation divided by the number of domains is a conversion-step curve [6, 29]. This illustrates the idea of computing the conversion-time curves in terms of random tessellations. Technical details and the numerical algorithm have been described in [30].

**Table 1** Conversion-step function for the central domain of Fig. 5

$s$	$N(s)$	$a(s)$
0	1	0.117
1	9	0.065
2	25	0.180
3	49	0.353
4	80	0.576
5	107	0.770
6	122	0.878
7	133	0.957
8	139	1.000

Discrete random tessellations are tractable only numerically. The simplest case is when all nuclei appear simultaneously (Voronoi tessellations). For this reason we will use experimental data for which practically simultaneous formation of nuclei has been reported [9, 12].

To compute the conversion-time curve in terms of random tessellations, we need to know the density  $\lambda$  of nuclei. In [8–11] the poor reproducibility of this parameter is reported and no particular values are given. From the data available it may be estimated as follows. Denote the total conversion as  $A(t)$ , and the conversion within one irreducible crystal plate as  $\alpha(t)$ . Within the description layer-by-layer, the total conversion is the sum of  $\alpha(t)$  functions over all irreducible plates

$$A(t) = \sum_{i=1}^N \alpha(t - i\zeta) \quad (3)$$

where  $N$  is the number of irreducible plates in a single crystal,  $\zeta$  is the time required for the reaction interface to propagate from the given plate to the next one (in Fig. 2 it equals 3 steps, i.e.  $\sim 10^{-2}$ – $10^{-3}$  min). The number of plates  $N$  may be estimated from

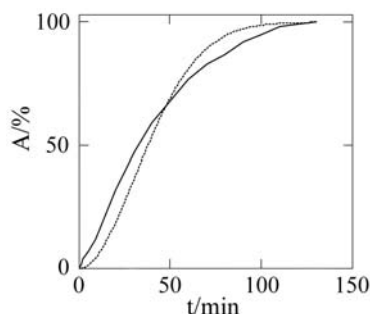


**Fig. 6** Experimental (solid) and calculated (dotted) conversion-time curves for  $\text{NH}_4\text{HCO}_3$  thermal decomposition ( $80^\circ\text{C}$ ,  $10^{-2}$  Pa)

the crystal thickness [9] as  $\sim 10^5$ . The inflection point on the experimental  $A_{\text{exp}}(t)$  curve [8] is at  $t = 9$  min. From relationship (3) the point of inflection of the  $\alpha(t)$  curve is estimated as  $t \sim 5$  min. Thus, we need to compute a random tessellation with the inflection point on conversion-time curve at step  $s \sim 10^3$ . The  $A(t)$  curve computed using numerical procedure [30] is shown in Fig. 6.

#### *Hierarchical kinetic model*

The nature of the reactions considered is such that chemical regularities manifest themselves in the observed kinetic behaviour indirectly, breaking through the universal geometrical regularities of the growth and impingement of nuclei. Conventional geometric-probabilistic models are macroscopic ones and adapted for describing only the latter regularities. With respect to them, chemical regularities are more microscopic; in other words, they belong to a deeper level of the micro-macro hierarchy. The approach suggested aims to discern chemical regularities through more macroscopic geometrical regularities. The conversion-time curve in Fig. 6 has been computed proceeding from microscopic assumptions. The main steps are as follows.

The mechanism of the reaction is assumed to be proton transfer, and from an examination of the  $\text{NH}_4\text{HCO}_3$  structure an assumption has been made as to which proton is transferred.

The crystal structure of  $\text{NH}_4\text{HCO}_3$  has been represented in terms of planigons and irreducible crystal plates. With the account of above assumptions, planigons have been constructed for conjugated  $\text{NH}_4\text{-HCO}_3$  pairs: each planigon represents two conjugated pairs.

The advance of the reaction front has been separated into the advance along the surface and into the bulk. The former is described as the propagation of the reaction from a nucleus to adjacent planigons. This means that kinetics of the reaction is represented in terms of the crystal structure of the solid reactant.

Impingements of randomly situated negative crystals are described in terms of random tessellations formed by planigons. The conversion-time curve is computed in these terms. Note that the metric of the random tessellation and parameters of discreteness are uniquely determined by the  $\text{NH}_4\text{HCO}_3$  crystal structure. In this way the

chemical individuality of the solid reactant manifests itself on a more macroscopic scale of nuclei impingements.

The model constructed is a hierarchical one in contrast to purely macroscopic conventional geometric-probabilistic models. Assumptions concerning proton transfer and equal probability for definite atoms to enter the reaction are microscopic assumptions. In generalizing them onto the macroscopic level, the use is made of the fact that both planigon tessellations and random tessellations are Dirichlet tessellations, though of different scale. This formal aspect is discussed in detail in [3-5]. This means the possibility to agree both microscopic and macroscopic levels in one and the same mathematical terms and to compute the conversion-time curve proceeding from microscopic assumptions.

The computed conversion-time curve is shown in Fig. 6 together with the experimental curve [8]. Strictly speaking, this is not the comparison of these curves since one important parameter, nuclei density  $\lambda$ , has been estimated from experimental kinetic data. For the comparison in the strict sense it must be known before computations. Still it may be concluded that the model gives a reasonable curve. Note in this connection that only the simplest variants are considered in this paper to illustrate the approach. Further detailing of the model is possible at practically all stages, provided that this is justified by available experimental data. The crystal structure may be represented in terms of planigons in more detail; more versatile rules may be suggested for describing the nucleation in terms of planigon tessellation cellular automata; random tessellations may be constructed for nuclei of different age, etc. In a word, a 'zero approximation' is presented in the paper and the fit may be adjusted in the number of ways. But there is one material restriction. The inflection point in the experimental curve corresponds to  $A_{\text{exp}}=12.8\%$ . This is not in agreement with the mechanism of nucleation and growth to impingement. In terms of random tessellations  $A_{\text{max}}$  is about 35 to 45%. The same estimate is obtained for the Avrami-Erofeev rate equation:  $\alpha_{\text{max}}=0.4$  for  $n=2$  and  $\alpha_{\text{max}}=0.29$  for  $n=3$ ; irrespective of  $k$ . The model curve in Fig. 6 falls within this range (37%). It is very important that this requirement of the model is supported by experimental estimations for  $A_{\text{max}}$  in the range 30-40% [11]. The conclusion is that the fit may be considerably improved, but counter-efforts of experimenters are needed. Without this a further adjustment is not justified.

## Conclusions

The model suggested is a first attempt to describe the kinetics of crystallysis reactions in chemical terms of the crystal structure and elementary events. The model is based on experimental observations for specially prepared plate-like single crystals of  $\text{NH}_4\text{HCO}_3$ . It illustrates previously suggested discrete approach [3-7] using a simplest example that a theorist may find within the discussed class of reactions. This approach is an extension of rather than an alternative to the conventional geometric-probabilistic approach [4]. As conventional models, the model suggested describes the formation of nuclei and their growth to impingement. In contrast to conventional models, it provides the room for representing the crystal structure of a solid reagent

and elementary events. Accordingly, it is much more involved. Intuition of a chemist tells that such models as Avrami–Erofeev rate equation are too simple to be adequate in all respects. They may be good enough if we are ready to restrict ourselves with only geometrical regularities of the reaction front advance on the macroscopic scale, but hardly suitable if a more subtle insight into the mechanism is the aim. More simple homogeneous reactions are described by models the mathematical structure of which is more complicated. The main aim of this paper is to show the principle possibility of developing models in this respect. Among disparate aspects of kinetic data analysis discussed in the current literature [31–37], this aspect gets an insufficient attention. The model proceeds from two microscopic assumptions and result in the acceptable conversion-time curve. It may be detailed in a number of ways, but more experimental information is required as the basis for this. Further development of the approach requires examination of carefully prepared single crystals (first of all, plate-like ones) with as well-characterized faces as possible. Modern experimental techniques available provide in this respect more possibilities than are used in the field. Reactions proceeding with the formation of only gaseous products are of especial interest at the first stage.

## References

- 1 A. K. Galwey and M. E. Brown, *J. Therm. Anal. Cal.*, 60 (2000) 863.
- 2 V. Kohlschutter and M. Luthi, *Helv. Chim. Acta*, 13 (1930) 978.
- 3 A. Korobov, *Heterog. Chem. Reviews*, 3 (1996) 477.
- 4 A. Korobov, *J. Math. Chem.*, 24 (1998) 261.
- 5 A. Korobov, *Discrete Dynamic in Nature and Soc.*, 4 (2000) 165.
- 6 A. Korobov, *J. Math. Chem.*, 25 (1999) 365.
- 7 A. Korobov, *J. Thermal Anal.*, 44 (1995) 187.
- 8 E. A. Prodan, M. M. Pavluchenko and T. N. Samoseiko, *Proc. Byelor. Acad. Sci., Ser. Chem.*, 2 (1970) 24 (in Byelorussian).
- 9 E. A. Prodan, M. M. Pavluchenko and T. N. Samoseiko, *J. Phys. Chim.*, 46 (1972) 2653 (in Russian).
- 10 E. A. Prodan, M. M. Pavluchenko and T. N. Samoseiko, *Kinet. i Katal.*, 15 (1974) 796 (in Russian).
- 11 *Heterogeneous Chemical Reactions*, E. A. Prodan Ed., Nauka i Technika, Minsk, 1979 (in Russian).
- 12 E. A. Prodan, *Topochemistry of Crystals*, Nauka i Technika, Minsk, 1990 (in Russian).
- 13 T. Loertin, C. Trautmann, R.T. Kroemer et al., *Angew. Chem. Int. Ed.*, 39 (2000) 891.
- 14 B. N. Delone, N. P. Dolbilin and M. P. Shtogrin, *Proc. Math. Inst. Acad. Sci. SSSR*, 148 (1978) 109 (in Russian).
- 15 B. Grunbaum and G. C. Shephard, *Tilings and Patterns*, San Francisco, Freeman, 1987.
- 16 B. K. Vainshtein, *Modern Crystallography, Foundations of Crystallography*, Springer Verlag, 1980.
- 17 A. Okabe, B. Boots, K. Sugihara and S. N. Chiu, *Spatial tessellations: Concepts and applications of Voronoi Diagrams*. New York, Wiley, 1999.
- 18 F. Pertlik, *Tschemaks Mineralogische und Petrographische Mitteilungen*, 29 (1981) 67.

- 19 A. Korobov, *Internet J. Chem.*, 5 (2002) 8.
- 20 International Tables for X-ray Crystallography, N. F. M. Henry and K. Lonsdale Eds., Vol. 1, International Union for Crystallography, 1952.
- 21 A. Korobov, *Thermochim. Acta*, 279 (1996) 191.
- 22 F. Bechstedt and R. Enderlein, *Semiconductor Surfaces and Interfaces, their Atomic and Electronic Structures*, Akademie-Verlag, Berlin 1988.
- 23 N. Koga and H. Tanaka, *Thermochim. Acta*, 388 (2002) 41.
- 24 A. Korobov, *Thermochim. Acta*, 254 (1995) 1.
- 25 I. Langmuir, *J. Amer. Chem. Soc.*, 38 (1916) 2221.
- 26 A. Korobov, *Complexity*, 4 (1999) 31.
- 27 V. Z. Belen'kiy, *Geometric-Probabilistic Models of Crystallization*, Nauka, Moscow, 1980 (in Russian).
- 28 D. Stoyan, W. S. Kendall and J. Mecke, *Stochastic Geometry and its Applications*, Chichester, Wiley, 1996.
- 29 A. Korobov, *Functional Mater.*, 6 (1999) 620.
- 30 A. Korobov, *Bull. Kharkov Nation. Univ., Chemistry*, 26 (1999) 44.
- 31 N. Koga, J. M. Criado and H. Tanaka, *J. Therm. Anal. Cal.*, 67 (2002) 153.
- 32 M. Maciejewski, *Thermochim. Acta*, 355 (2000) 145.
- 33 F. Rodante, G. Catalani and S. Vecchio, *J. Therm. Anal. Cal.*, 68 (2002) 689.
- 34 A. K. Galwey, *Thermochim. Acta*, 397 (2003) 249.
- 35 B. Malecka, E. Drozd-Ciesla and A. Malecki, *J. Therm. Anal. Cal.*, 68 (2002) 819.
- 36 A. Ortega, *Int. J. Chem. Kinet.*, 33 (2001) 343.
- 37 K. S. Khairou, *J. Therm. Anal. Cal.*, 69 (2002) 583.